Franco F. Orsucci
Nicoletta Sala
Editors

Complexity Science in Human Change

NOVA

Chapter 5

An Experimental Verification of NeuroPhysics Treatment by Executing a Multifractal Analysis of Surface Electromyography Signals on Trapezius, Abdominals, and Adductor Muscles in Athletes

Calogero Rinzivillo[1]
Ferda Kaleagasioglu[2,3,*]
Francesco Casciaro[4]
Fabio Scoppa[5]
Riccardo Marvulli[6]
Ken Ware[7]
Elio Conte[3]
and Antonio Di Ieva[8]

[1]Department of Medical-Surgical Sciences and Advanced Technologies, Medical School and Policlinic, University of Catania, Italy
[2]Department of Pharmacology and Clinical Pharmacology, Faculty of Medicine, Istinye University, Istanbul, Turkey
[3]School of Advanced International Studies on Applied Theoretical and Non-Linear Methodologies of Physics, Bari, Italy
[4]Department of Oncology and Internal Medicine, University Aldo Moro, Bari, Italy
[5]Faculty of Medicine and Dental Surgery, Sapienza University of Rome, Rome, Italy
[6]Department of Basic Science, Neuroscience and Sense Organs, University Aldo Moro, Bari, Italy
[7]Institute Neurotricional Sciences Pty. Ltd., Gold Coast, QLD, Australia

[*] Corresponding Author's Email: ferda.kaleagasioglu@istinye.edu.tr.

In: Complexity Science in Human Change
Editors: Franco F. Orsucci and Nicoletta Sala

[8]Computational NeuroSurgery (CNS) Lab, Macquarie Medical School,
Faculty of Medicine, Health and Human Sciences, Macquarie University,
Sydney, Australia

Abstract

Background: NeuroPhysics Treatment (NPT) is an exercise-based approach that was hypothesized to utilize the body's genius to trigger and organize self-healing. NPT involves mild resistance training exercises with extremely slow movements in an erect posture under therapeutic coaching. NPT was hypothetically based on system dynamics, chaos, and fractal theory. The aim of this study was to investigate this thesis by a cross-disciplinary approach.

Methods: The differences between surface electromyography (sEMG) signals recorded on the trapezius, the abdominals, and the adductors of 10 healthy, male athletes at rest, during and following NPT were investigated by using the multifractal analysis based on Multifractal Detrended Analysis and with added Surrogate Data Analysis.

Results: All the muscles represent complex systems, and their bio signal profiles constitute a multifractal. During the NPT treatment, these systems are subjected to continuous and differential transitions, enabling a continuous and differential rearrangement of the indices between different muscles and in the same muscles.

Conclusions: This study is methodological and evidences the importance of always performing the multifractal analysis in sEMG studies and indicates the necessity for the same analysis of the EEG and of the R-R signals to obtain a whole picture of the involved dynamics, as a future prospect.

Keywords: surface electromyography, multifractal analysis, detrended fluctuation analysis, NeuroPhysics treatment

1. Introduction

EMG signals display complexity which can be quantified by the fractal theory [1, 2]. Recent research suggests that fractal dimension may be considered as a reliable EMG parameter and is not dependent on the exerted force. [3]. Additionally, fractal analysis has been suggested to have huge potential for wide application in the study of the impact of various stimuli on biosignals, including ECG and EEG and these analyses are very important in

physiological and sports sciences paving the way for better understanding of human physiology [1].

In 2013, Ross and Ware published a paper relative to NPT, that was practiced and originated by Ware, based on system dynamics, chaos, and fractal theory [4]. The authors established a theoretical point of view regarding fractal physiology principles for this treatment without elaborating on their experimental data based on surface electromyography (sEMG), electroencephalography (EEG) and heart rate variability (HRV) analyses. The aim of the present paper, which is methodological in principle, is to fill in the experimental gap through the illustration of Ross and Ware into the theoretical treatment by introducing the principles of multifractal theory and by studying the series of experimental data of surface electromyography accompanied by multifractal analysis. The data have been obtained by simultaneously recording the sEMG, the EEG, and the ECG at 1000 Hz of sampling frequency and the analysis of the data has been obtained by performing a multifractal analysis using MATLAB software based on DFA (Detrended Fluctuation Analysis) of the arising time series data. Ten athletes were used for the analyses, all clinically controlled in their fundamental parameters. sEMG, EEG and ECG were performed with the recording of the relative signals at 1000 Hz. In the present paper, we will present the results related to the sEMG. In the following paper, we will deal instead with the results related to the EEG and the R-R signal. We carried out our analysis by means of the Detrended Fluctuation Analysis (DFA) accompanied by the analysis of surrogate data and statistical analysis on the various subjects. A conclusive interpretation of the physiological and clinical profiles is reported.

The purpose of this chapter is twofold. On the one hand, we invite the readers to use multifractal analysis in sEMG teaching them what to do. On the other hand, we suggest the reader to consider the validity of the NPT method that is based on fractal theory and chaos theory and thus it represents a good occasion to study multifractals. NPT is a method that, as explained in the section Theoretical Background, is based on chaos theory, on the multifractality of the temporal sets that emerge from the study. It is shown that the use of multifractality is a very powerful method that can be used safely by the researcher and on the other hand, it is also shown that the indices emerging from these studies, such as the Generalized Hurst Exponents and the other indices that are introduced in this work, and which arrange themselves well during the study, constitute a valid element of analysis and clinical diagnosis and therefore function quite well in every respect.

1.1. Theoretical Background

The historical background of this paper is reported in the article by Ross and Ware [1] which we refer to since it exposes in rigorous detail every clinical aspect regarding NPT treatment on the subject. In particular, the following facts were observed: (1) rapid, involuntary muscle contractions and relaxations, (2) mild and/or vigorous fluctuations in limbs or torso, (3) mild and/or vigorous chaos or periodic patterns in one or more jointed regions, and (4) abrupt changes in activity location, symmetries, velocity, and in-phase/anti-phase relations.

Introducing a new paradigm in the delivery of psychophysical therapy that has relevance to our greater understanding of how the nonlinear dynamical system is perceived and interacts with the environment at highly discrete scales.

For decades, NPT has been attributed to unprecedented highly positive health and wellbeing transitions in very small-time scales for patients who presented with highly complex neurological diseases and disorders deemed untreatable by the present medical paradigm, inclusive of incomplete and complete spinal cord injuries. Other conditions benefiting from NPT include motor neuron disease, multiple sclerosis, Graves' disease, lupus and migraine [1]. The said NPT outcomes have been well documented and publicized by the international and national media. https://www.neurophysicstherapy.global/media/

1.2. The Vital Importance of Scientific Research into NPT Phenomena

It is to be understood that scientific research surrounding NPT is a reverse engineering process. A phenomenon displaying enormously beneficial qualities has been discovered, firstly, and now we need to understand why this is the case from a scientific perspective; That is, what are we observing, how can this new knowledge be transferred towards the greater understanding of what is happening in other nonlinear dynamical systems and do present-day theories surrounding nonlinear dynamical systems need to be expanded upon as a result of this new knowledge.

Observing and measuring a human system during these phases enables the observer to visually appreciate the CNS's relationship with the environment, its perception of the environment, its extreme sensitivity to initial conditions,

self-organized criticality, and the ability to recognize the signatures of a system harboring disease or disorder in the absence of knowledge of medical records, when compared to the signatures of a healthy robust system. Obviously, there is a lot of knowledge missing in other fields of the medical and physical sciences, as other fields of medical science have yet to produce such outcomes.

1.3. Systems-Wide Phase Transitions and Their Importance to the Future Health, Wellbeing, and Psychophysical Function of the Human Nervous System

Terms such as phase transitions are generalized terms that summarize a multitude of events taking place in dynamical systems. However, these terms may be used in context to express the sudden shifts in behavior during NPT observed in these systems in phase space.

During all stages of NPT, individuals are perfectly coherent and are able to communicate and start/stop the observed transition dynamics at will, as with all other individuals who have learned how to transcend the levels of normal inhibition of the human system displays to control the underlying chaotic state of the central nervous system - not eliminate chaos, as this is needed to enable us to seamlessly transition between mental states and adapt rapidly to changes in the environment. It is when the brain becomes less chaotic that pathologies such as seizures occur to enable the system to dispose of its excess energy and over-orderliness.

The connection with chaotic theory, chaotic transitions, dynamics of these chaotic transitions, fractality, and multifractality of these EMG systems were also discussed in Ross and Ware's article in detail [4] but a connection between theory and experimental aspects was missing that instead is discussed in the present paper. For the sake of brevity, we refer the reader to this article and other selected bibliographic references of this content [4–23], which we recommend the reader to read very carefully because in this way, he/she will obtain a complete exposition and exhaustive understanding both from a clinical and theoretical point of view. For our present work, we only add that the link between the EMG signals and multifractality is expressed very well in the work of Ross and Ware and we have fully adopted that in the present work. In particular, Ross and Ware expressed the following convictions: The general explanations of the patterns observed above are well established. They are fixed in the nonlinear dynamical nature of complex systems. As one

deduces from Haken's theory of non-equilibrium phase transitions, the tendency of such EMG systems is to be in the regime of instability [6]. The loss of stability is outlined by the appearance of new behavioral patterns [7]. Different patterns represent different attractors. These changes are chaotic transitions [6,8] and this means that the result is a new attractor.

The psychophysical system is attracted to certain states to innately maintained patterns of behavior that have a desirable amount of degrees of freedom in the best interest of survival and adaptation to changes within the environments. The innate system has no preference or bias so when there is a change in behavior associated with a disease or disorder then these behaviors are maintained within a rogue metabolic attractor that has limited degrees of freedom. When these patients' systems expose their underlying kinetics, these kinetics display highly deterministic and very regular periodicity. They appear to be stuck in this rouge attractor that can be dimensionally and metabolically measured and are visually constructed via the EMG signals. These systems need a prescribed perturbation which occurs via the NPT process to input more energy and information into the system, so that the system can build up the escape velocity needed to pull out of the rogue attractor, and this would be displayed as phase transitions where the system will then display systems wide flowing movements similarly to flocks of birds flying in unison. This is what occurs and the system exhibits rapid enhancements to function and performance when this occurs. A healthy person's system will display these flowing movements all the time.

The studies of multifractals and chaos are linked in many ways. They share common ideas and methods of analysis. From a methodological point of view, we argue that a systems phase space (set) may be formed from the time series data. When the phase space system is fractal the system that generated the time series is chaotic. The fractal time dimension of the phase space informs us of the minimum number of independent variables that are required to generate the time series. Chaos indicates that the output of a deterministic nonlinear process is so complex that it mimics the random behavior, the point being that chaos analysis is to determine if the experimental data are due to a deterministic or random process and, if this is due to a deterministic process to determine the mathematical kind of that process. The essential properties of a chaotic system are that it is deterministic dynamical system, it is described either by difference or differential equations, it has a strange attractor where, as noted previously, the technical jargon word chaotic means that the system has sensitivity to initial conditions and the word strange means the attractor is

fractal. Such fractal dimension is related to the number of independent variables that are needed to generate the time series of the values of variables, it has bifurcations that happen when the form of the trajectory in the phase space changes a parameter passing through a certain value, control that means that small changes in such parameters produce small changes in the subsequent values of the variables. In nonlinear systems, small changes in such parameters produce enormous changes in the subsequent values of the variables because of the dependence to the sensitivity to the initial conditions.

All the previous statements are theoretical elaborations designed in the paper mentioned above [4]. In the present paper, we give indication that the experimental time series, data recorded by sEMG on the examined athletes, are multifractals.

2. Materials and Methods

2.1. Participants

Ten subjects who were male athletes participated in the research. The age of the subjects varied from 19 to 23 years old. Their BMI varied between 22- 25 and their height was between 175 and 180 cm.

The training of such athletes consisted in continuous workouts and Nutritional and Fitness programs supporting such athletes to improve their skills.

Trained athletes were confirmed by ECG, the R-R signal, by the BMI performed by the impedance meter and by lipid echography. All such measurements were performed by our group in addition to other exams performed by our clinicians. All the athletes were submitted to polygraphy analysis.

All the athletes signed an informed consent for the treatment. The health conditions of the subjects were constantly monitored by a group of clinicians during the rest, the treatment by NPT, and the post-treatment phases to evaluate the subjective conditions of the athletes. For at rest, we intend the athletes with muscles at rest but with their autonomous system activated and at alert and thus always ready to be activated, in order to respond to the external stimuli.

2.2. sEMG Recordings and Analysis

All sEMG signals were simultaneously recorded using BioRadio®150 technology (Great Lakes Neurotechnologies, Cleveland, OH, USA) samples at 1000 Hz for the frequency of recording. Such analysis was performed at rest, during NPT and post NPT. The following muscles were selected for the sEMG: right and left trapezius, right and left abdominals, and right and left adductors of the lower limbs. Recordings were also taken during NPT while lying on the floor. A time of 5 minutes was selected for at rest treatment and post treatment analysis.

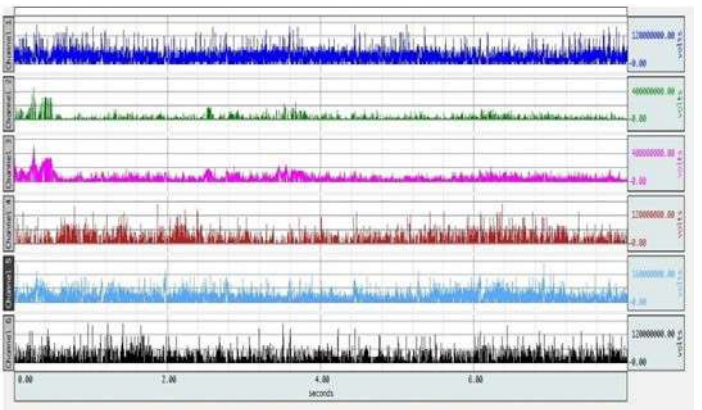

Figure 1a. The recording of sEMG for right trapezius for a time of about 8 seconds. Clinical condition: At rest.

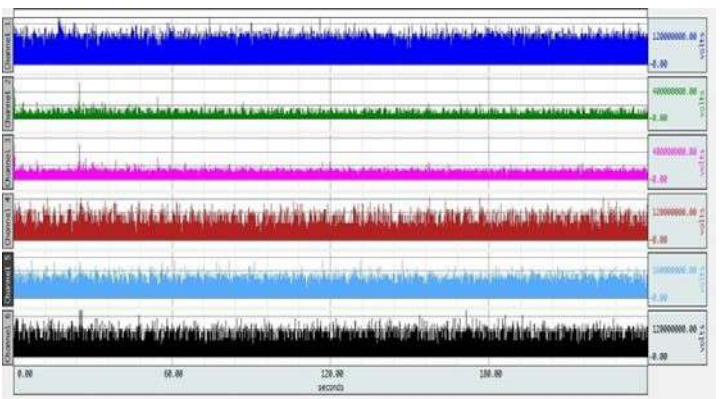

Figure 1b. The recording of sEMG for right trapezius for a time of about180 seconds. Clinical condition: At rest.

The examinations consisted of recording 8 signals arising from six sEMG channels (see Figures 1-3 for the relative signals that relate the recording of the signal at rest before the treatment, during the treatment and post the treatment. Each figure relates the recording of the sEMG signals for the time period of 8 and 200 seconds). The figures are reported in Figures 1a,b; 2a,b;3a,b.

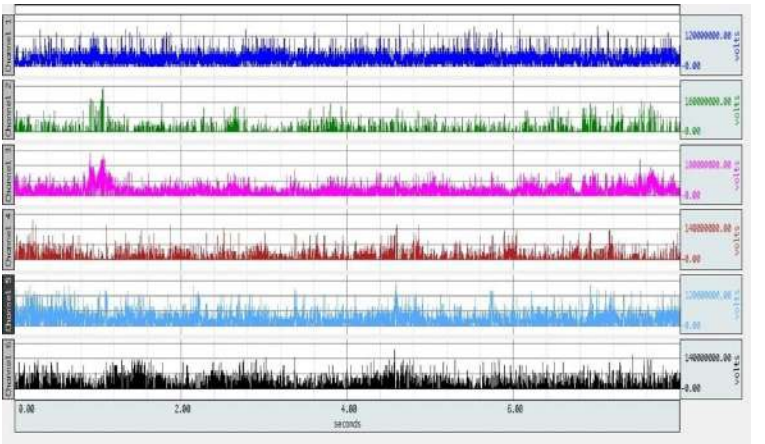

Figure 2a. The recording of sEMG for right trapezius for a time of about 8 seconds. Clinical condition: During NPT.

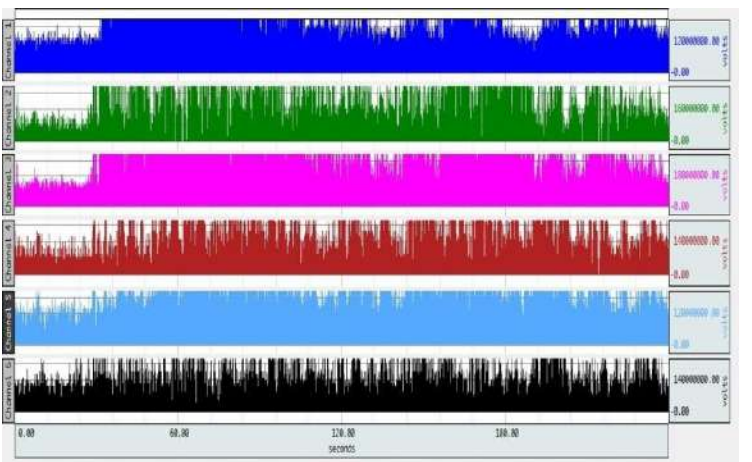

Figure 2b. The recording of sEMG for right trapezius for a time of about 180 seconds. Clinical condition: During NPT.

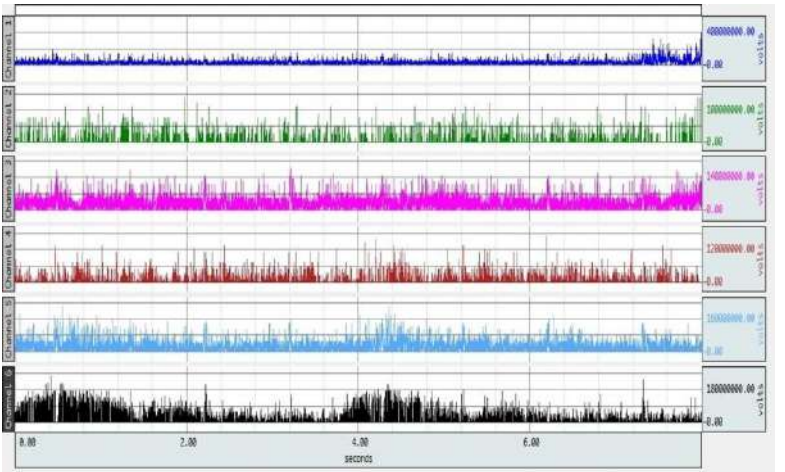

Figure 3a. The recording of sEMG for right trapezius for a time of about 8 seconds. Clinical condition: Post-NPT.

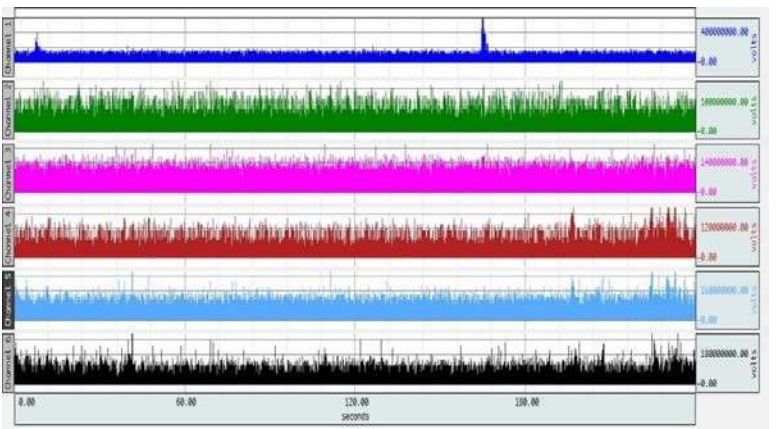

Figure 3b. The recording of sEMG for right trapezius for a time of about 180 seconds. Clinical condition: Post-NPT.

The electrodes were placed lengthwise on the right and the left trapezius for channels 1 (Ch1) and 2 (Ch2), respectively. These regions were selected because the trapezius is highly reactive to activation of the sympathetic nervous system (SNS). Any significant differences between tone and synchronization between the left and right trapezius are indicative of undesirable hemisphere dominance whereas dominantly stable bilateral synchronization is observed in healthy men and women [24, 25].

For the EMG recording of channels 3 (Ch3) and 4 (Ch4), the electrodes were placed on the right and the left abdominals, respectively, bilaterally adjacent to the navel.

The electrodes were placed lengthwise on the adductors of the lower right and the lefty limbs (legs) for channels 5 (Ch5) and 6 (Ch6), respectively.

Placing the EMG electrodes on these three muscles (trapezius, abdominals, and adductors), enabled to monitor the overall system responses.

We used raw data. The sample frequency was 1000,00 Hz and the analysis was extended on the whole 5 minutes signal. Subsequently, each time series arising from one of the six channels was elaborated in the MATLAB software for the Detrended Fluctuations Analysis as developed by Wang et al. [26] and the indices h(q), τ(q), α(q), f(α), D(q) were estimated.

2.3. How to Perform the Methodological Analysis: Theoretical Elaboration

All the arising sEMG time series data were stored on a computer. The procedure of the analysis of the data was developed via a multifractal analysis (MF-DFA 1-D) following the method indicated by Wang et al. [26]. We have six steps of analysis:

Step 1

We calculated the function

$$y(k) = \sum_{t=1}^{k} [x(t) - \bar{x}(t)], k = 1,2, \dots \dots, N$$

of the fluctuations between the experimental time series, $x(t)$ and its mean value $\bar{x}(t)$.

Step 2

The function $y(k)$ was divided in $N_s = N/s$ not overlapping segments all having the same length s.

Step 3

The local trend $y_v\ (i)$ was estimated by using the least squares method for each segment.

Since the detrending of each temporal series was obtained by subtracting the polynomial fits from $y(i)$, we estimated $y_v(i)$ by the relation

$$y_s(i) = y(i) - y_v(i)$$

Step 4

We evaluated the "local trend" for each of the $2N_s$ segments by using the least square fit of the series. This is a procedure that finds the best fit behavior respect to a series of points by minimizing the sum of the residuals. The variance was determined in the following manner

$$F^2(s,v) = \frac{1}{s}\sum_{i=1}^{s} y^2[(v-1)s+i]\ , v = 1, 2, \ldots\ldots, N_s$$

with

$$F^2(s,v) = \frac{1}{s}\sum_{i=1}^{s} y^2[N-(v-N_s)s+i]$$

for

$$\nu = N_S+1, 2, \ldots. 2N_S$$

Step 5

By executing the mean on all the segments, we obtained the function of the fluctuations of order q

$$F_q(s) = \left[\frac{1}{2N_s}\sum_{v=1}^{2N_s}[(F^2(s,v))^{q/2}]\right]^{1/q}$$

with q assuming any value except zero.

For q = 0, we have instead

$$F_{4N_s}(s) = exp\left[\frac{1}{0}\sum_{v=1}^{2N_s} ln[F^2(s,\nu)]\right]$$

Such generalized functions of fluctuations, $F_q(s)$, are q dependent and are correlated with s for various q. This objective is reached by repeating steps 2-5 for the different time scales s.

Step 6

We determined the "scaling behavior" of functions of fluctuations by analysis of the behavior $Ln\ F_q(s)$ vs $Ln\ s$ for any q. In cases where the given time series $x(t)$ results are correlated in accordance with a *"long range"* law of power, $F_q(s)$ will increase by a power law at increasing values of s,

$$F_q(s)\ \mathrm{a}\ s^{h(q)}$$

These are the six steps of the work. Furthermore, due to its affinity with the Hurst exponent, $h(2)$ is called the generalize Hurst exponent. Generally speaking, we have a nonlinear behavior as function of q.

Other fundamental relations are

$$r(q) = qh(q) - 1$$

the generalized multifractal dimension

$$D(q) = \frac{c(q)}{q-1}$$

The Lipshits-Holder exponent

$$\alpha(q) = r'(q)$$

and the multifractal spectrum

$$f(\alpha) = q\alpha(q) - r(q)$$

This last observation completes the method that we developed by MATLAB. The index we used are given below.

$$\Delta\ \mathrm{h} = \mathrm{h}(q_{min})\text{-}\mathrm{h}(q_{max})$$

Since richer multifractality corresponds to higher variability of h(q), the degree of multifractality is quantified by this index.

In addition, we have

$$\Delta\alpha = \alpha_{max} - \alpha_{min}$$

$$\Delta\alpha_L = \alpha_0 - \alpha_{min}$$

$$\Delta\alpha_R = \alpha_0 - \alpha_{max}$$

where α_0 is the particular value of α corresponding to q = 0

$$\Delta f(\alpha) = f(\alpha_{min}) - f(\alpha_{max})$$

$$f(\alpha) = A(\alpha - \alpha_{max})^2 + B(\alpha - \alpha_{max}) + C$$

with A, B, C being the coefficients of the parable.

The other step is that one of the surrogate analysis that is able to convince us that we are in presence of a multifractal. This Surrogate Data Analysis (shuffled data) was used to test and to verify the multifractality of the experimental data and consisted in the analysis of $F_q(s)$, the Average Mutual Information and the multifractal spectrum $f(\alpha)$ of our data (see the Figures 4, 5, 6, 7).

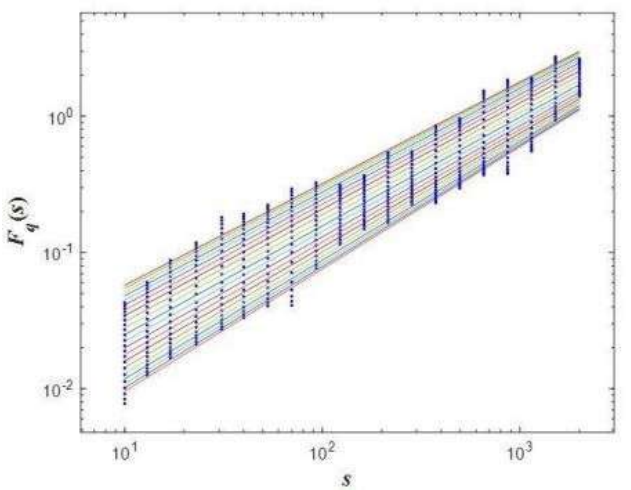

Figure 4. We report $F_q(s)$ against s to convince us that we are in presence of a multifractal.

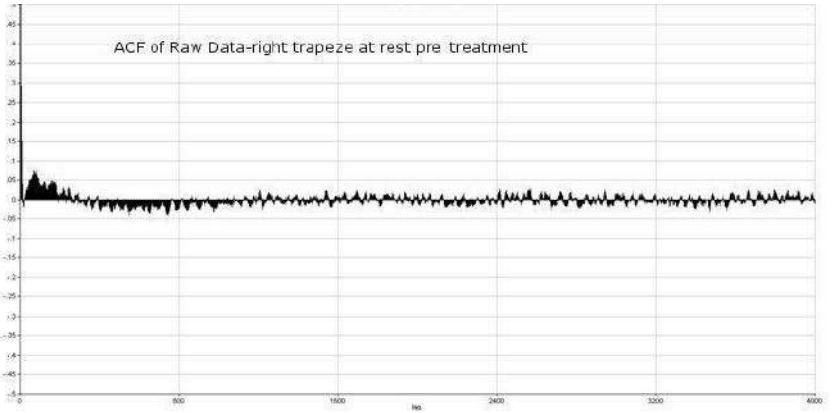

Figure 5. ACF of the shuffled data.

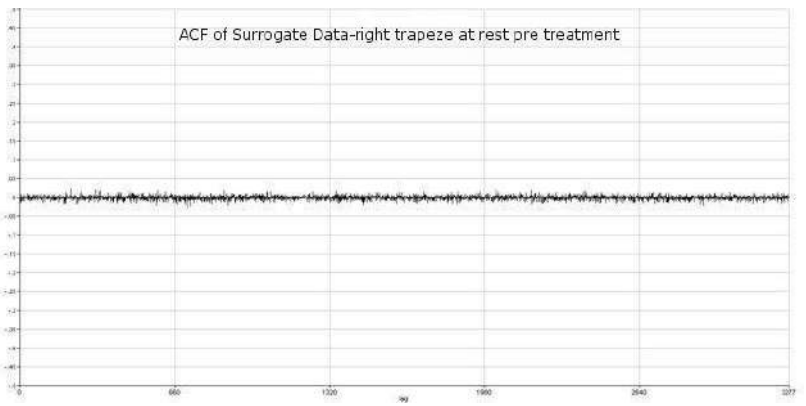

Figure 6. ACF of the shuffled data. The results confirm that we are in presence of a multifractal.

2.4. Statistical Analysis

After the proper verification for normality and sphericity, the Repeated-Measures ANOVA statistical analysis was used to compare the data of pre-, during- and post-NPT for each electrode. A p value less than 0.05 was considered as statistically significant.

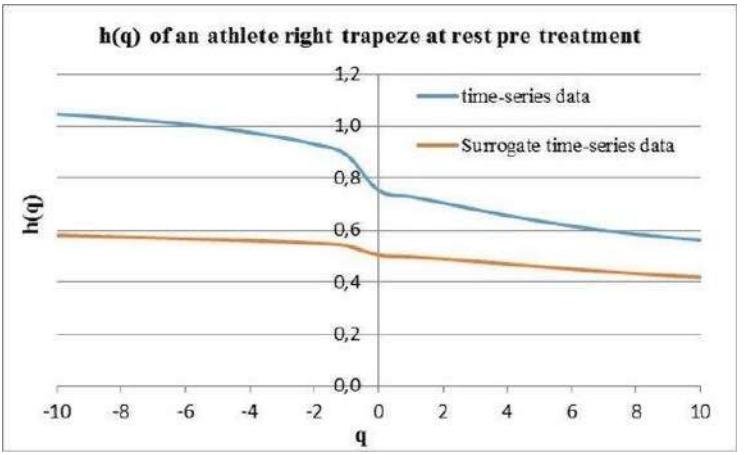

Figure 7. These results confirm that we are in presence of a multifractal.

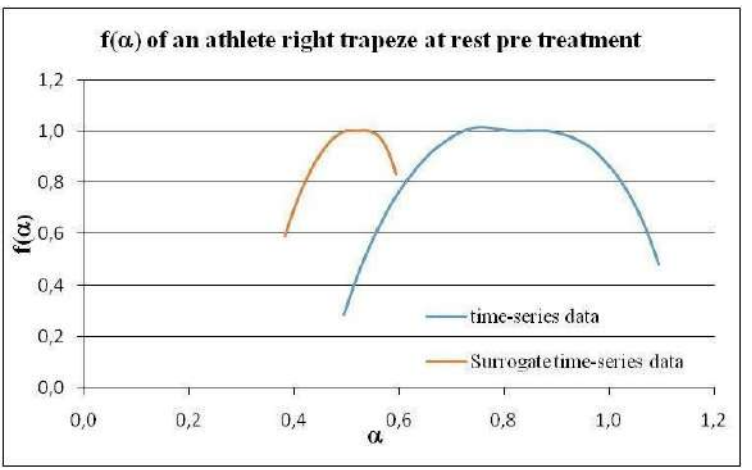

Figure 8. These results confirm that we are in presence of a multifractal.

3. Results

3.1. The Multifractal Analysis

For the multifractal analysis, the calculated indices h(q), D(q),τ(q), α(q), f(α), are shown in the Figures 9-13.

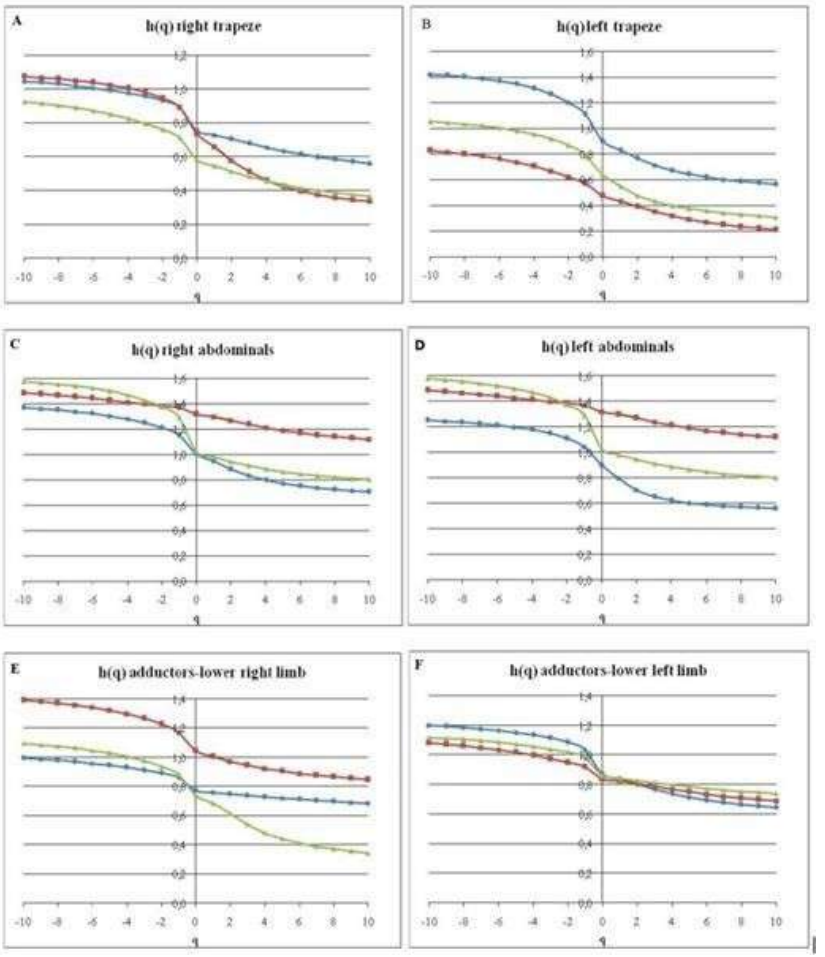

Figure 9. Representation of h(q) as function of q: The right (A) and the left (B) trapezius, the right (C) and left (D) abdominals and the right (E) and left (F) adductors of athletes at rest pre-( ), during-( ) and post-( )-treatment (at rest) are shown. We have the typical behavior of the multifractals dynamics in all the examined phases of pre-, during- and post-treatment: the whole of the exponents h(q) describes the scaling of the qth-order fluctuation function. Multifractality relates the scaling property of a time series that is represented by an array of scaling exponents, and not by any single one. The multifractality of a time series is identified by examining the dependence of h(q) on high and low-order moments. If the time series is monofractal, then h(q) is independent of q. If the series is multifractal, then h(q) depends on q, characterizing in this manner a single form of self-similarity over time. h(q) depends significantly on q only if large and small fluctuations scale differently. With major or minus difference, we find such a situation in the pre-, during- and post-treatment in all the examined cases.

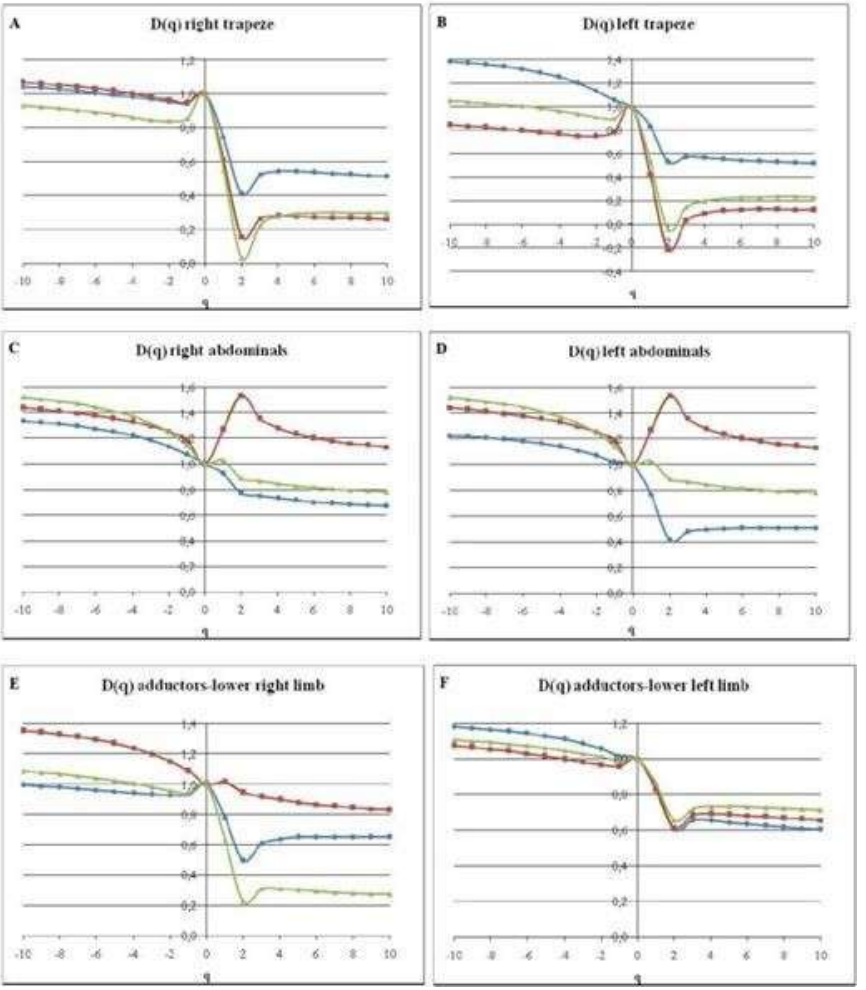

Figure 10. Representation of D(q) as function of q: The right (A) and the left (B) trapezius, the right (C) and left (D) abdominals and the right (E) and left (F) adductors of athletes at rest pre-( ), during-( ) and post-( )-treatment (at rest) are shown. Generally speaking, D(q) is a measure of the inhomogeneity or multifractality of an attractor whenever the D(q) values are not equal for all q. However, when the D(q) are the same, the distribution of vector points on the attractor is fairly homogeneous.
A chaotic attractor with non-constant values of the generalized dimension is called a multifractal. The results in this picture are therefore in line with the interpretation that signals of sEMG as we calculated them for trapezius, abdominals and adductors are time series of a multifractal.

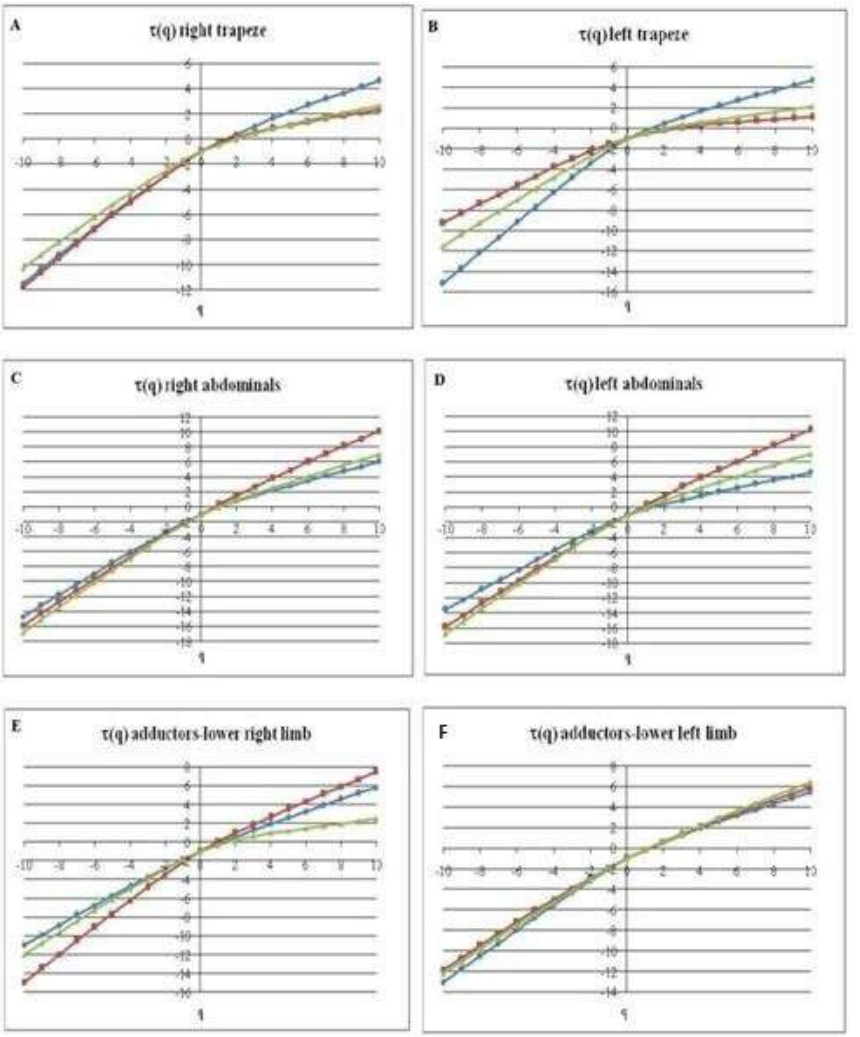

Figure 11. Representation of τ(q) as function of q: The right (A) and the left (B) trapezius, the right (C) and left (D) abdominals and the right (E) and left (F) adductors of athletes at rest pre-( ), during-( ) and post-( )-treatment (at rest) are shown. The h(q) obtained using MFDFA is related to the Rényi exponent τ(q) by the relation, previously introduced, $\tau(q)= qh(q)-1$.

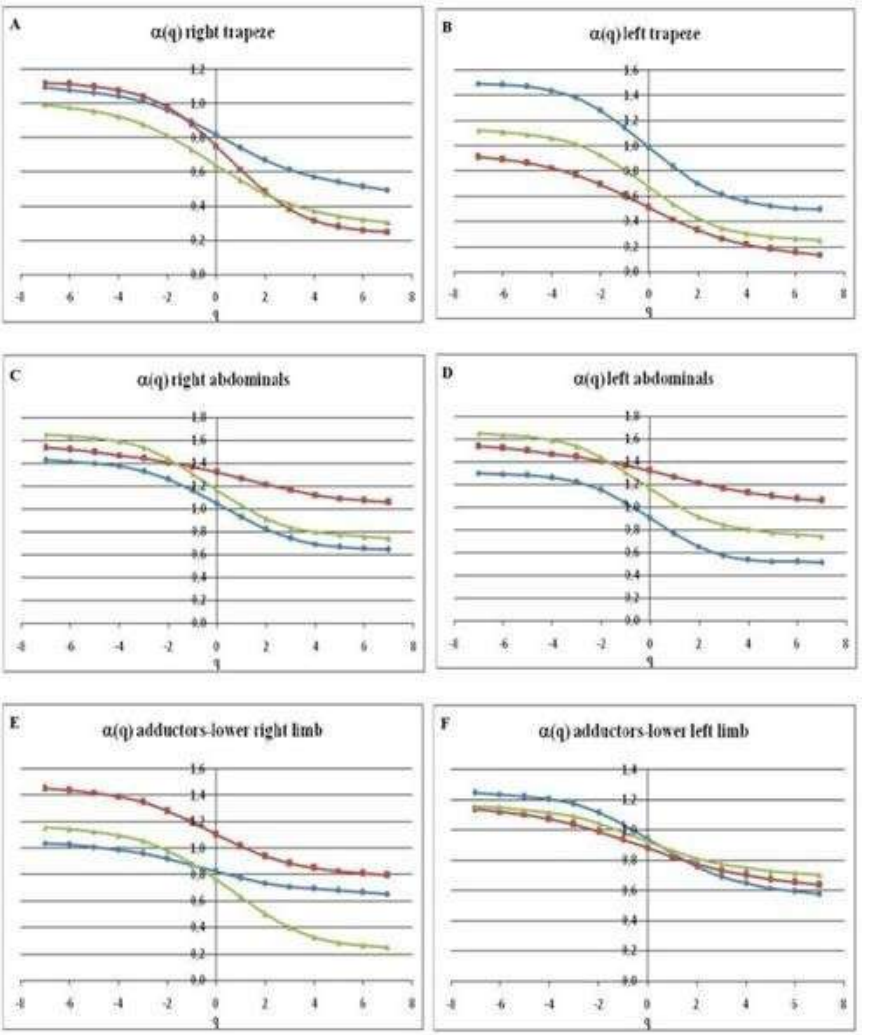

Figure 12. Representation of α(q) as function of q: The right (A) and the left (B) trapezius, the right (C) and left (D) abdominals and the right (E) and left (F) adductors of athletes at rest pre-( ), during-( ) and post-( )-treatment (at rest) are shown. α is the Hölder exponent or singularity strength, and it gives the multifractal spectrum *f*(α), which describes multifractal time series. For pure multifractals, the value of α decreases with increased fluctuation as it is obtained in these graphs for right and left trapezius, abdominals and adductors in condition at rest, pre- and post-treatment, as well as during the treatment.

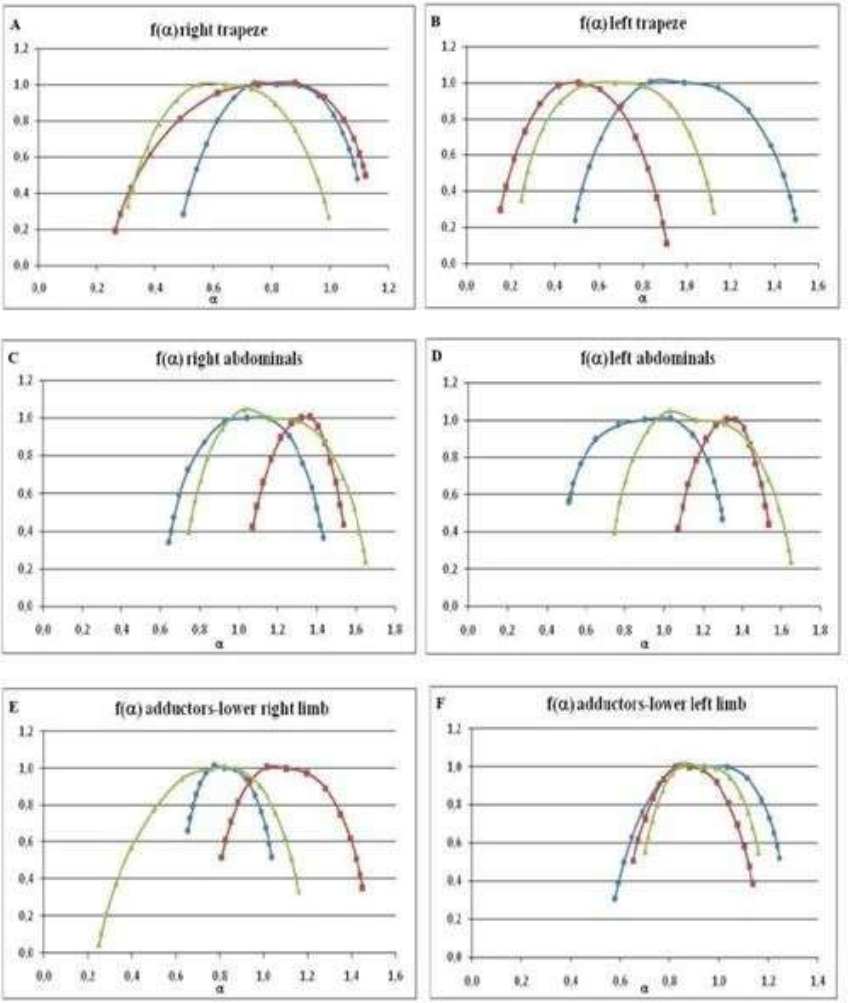

Figure 13. Representation of $f(\alpha)$, the multifractal spectrum, as function of α: The right (A) and the left (B) trapezius, the right (C) and left (D) abdominals and the right (E) and left (F) adductors of athletes at rest pre-( ), during-( ) and post-( )-treatment (at rest) are shown. In all cases, the multifractal spectra are quite asymmetrical with convex parables, which confirms that the time series for the six selected regions are multifractal, but to a varying degree, since the curves are all different. All of them reach the maximum value $f(\alpha)$ of 1, relating to the single dimension of the studied variables. When the spectra are compared, we observe that their shapes are different; consequently, all of the studied data sets are subjected to different high and low fluctuations.

Table 1. Mean values ± standard deviation of the generalized hurst exponent, h(2), Δα, Δf, the coefficients A, B, C, Δh, $\Delta\alpha_L$, $\Delta\alpha_R$, recorded by channels 1 (right trapezius) 2 (left trapezius), 3 (right abdominals), 4 (left abdominals), 5 (right adductors) and 6 (left adductors) pre-NPT treatment (color white), during NPT treatment (color green) and post-NPT treatment (color pink) at rest in the healthy male subjects (n = 10)

	H(2)	Δα	**Δf**	**Δh**	$\Delta\alpha_L$	$\Delta\alpha_R$	**A**	**B**	**C**
CHANNEL 1 (right trapezius)									
Pre-treatment	0,796 ± 0,084	0,512 ± 0,059	-0,336 ± 0,224	0,413 ± 0,050	0,304 ± 0,039	-0,207 ± 0,055	-8,281 ± 1,182	-3,472 ± 0,880	0,674 ± 0,161
During treatment	0,551 ± 0,026	0,696 ± 0,002	-0,375 ± 0,164	0,560 ± 0,023	0,412 ± 0,034	-0,284 ± 0,036	-5,798 ± 0,557	-3,418 ± 0,058	0,534 ± 0,004
Post-treatment	0,472 ± 0,047	0,846 ± 0,163	-0,051 ± 0,123	0,725 ± 0,169	0,439 ± 0,115	-0,407 ± 0,049	-4,064 ± 1,782	-3,200 ± 0,982	0,444 ± 0,134
CHANNEL 2 (left trapezius)									
Pre-treatment	0,669 ± 0,129	0,694 ± 0,169	0,175 ± 0,038	0,413 ± 0,050	0,304 ± 0,039	-0,207 ± 0,055	-4,212 ± 1,379	-3,024 ± 0,350	0,511 ± 0,040
During treatment	0,546 ± 0,160	0,444 ± 0,227	-0,149 ± 0,122	0,345 ± 0,193	0,237 ± 0,139	-0,207 ± 0,088	-14,66 ± 8,432	-4,991 ± 1,236	0,555 ± 0,075
Post-treatment	0,589 ± 0,167	0,957 ± 0,137	-0,076 ± 0,476	0,825 ± 0,099	0,503 ± 0,157	-0,454 ± 0,022	-2,894 ± 0,310	-2,692 ± 0,432	0,436 ± 0,093
CHANNEL 3 (right abdominals)									
Pre-treatment	0,947 ± 0,076	0,905 ± 0,267	0,103 ± 0,136	0,787 ± 0,241	0,434 ± 0,141	-0,471 ± 0,130	-3,518 ± 1,269	-3,078 ± 0,275	0,383 ± 0,103
During treatment	0,908 ± 0,090	0,742 ± 0,183	-0,079 ± 0,210	0,625 ± 0,151	0,385 ± 0,079	-0,357 ± 0,116	-4,831 ± 1,313	-3,240 ± 0,389	0,477 ± 0,223
Post-treatment	0,849 ± 0,133	1,034 ± 0,183	-0,007 ± 0,235	0,882 ± 0,151	0,512 ± 0,132	-0,522 ± 0,052	-3,166 ± 0,469	-3,260 ± 0,152	0,267 ± 0,031

	H(2)	Δα	Δf	Δh	$\Delta\alpha_L$	$\Delta\alpha_R$	A	B	C
CHANNEL 4 (left abdominals)									
Pre-treatment	0,970 ± 0,036	0,853 ± 0,090	0,208 ± 0,179	0,746 ± 0,074	0,391 ± 0,078	-0,461 ± 0,016	-3,190 ± 0,190	-2,972 ± 0,098	0,391 ± 0,014
During treatment	0,949 ± 0,128	0,479 ± 0,190	0,003 ± 0,147	0,397 ± 0,168	0,246 ± 0,106	-0,234 ± 0,091	-9,725 ± 5,281	-2,434 ± 3,699	0,593 ± 0,095
Post-treatment	0,903 ± 0,039	0,794 ± 0,181	0,043 ± 0,014	0,674 ± 0,161	0,389 ± 0,083	-0,405 ± 0,098	-4,240 ± 1,253	-3,311 ± 0,203	0,396 ± 0,104
CHANNEL 5 (right adductors)									
Pre-treatment	0,872 ± 0,057	0,373 ± 0,031	-0,108 ± 0,461	0,300 ± 0,028	0,200 ± 0,087	-0,174 ± 0,059	-10,93	-2,526 ± 3,934	0,679 ± 0,230
During treatment	0,618 ± 0,116	0,901 ± 0,228	-0,093 ± 0,355	0,765 ± 0,201	0,464 ± 0,169	-0,438 ± 0,063	-3,907 ± 1,194	-3,297 ± 0,626	0,384 ± 0,064
Post-treatment	0,727 ± 0,162	0,840 ± 0,095	-0,574 ± 0,402	0,691 ± 0,085	0,523 ± 0,016	-0,316 ± 0,110	-3,991 ± 0,135	-2,560 ± 0,843	0,590 ± 0,256
CHANNEL 6 (left adductors)									
Pre-treatment	0,873 ± 0,100	0,534 ± 0,187	-0,109 ± 0,147	0,440 ± 0,166	0,280 ± 0,117	-0,255 ± 0,070	-8,495 ± 4,328	-3,984 ± 0,968	0,576 ± 0,009
During treatment	0,733 ± 0,128	0,722 ± 0,174	-0,398 ± 0,231	0,598 ± 0,151	0,426 ± 0,129	-0,296 ± 0,052	-5,402 ± 2,400	-3,069 ± 0,777	0,600 ± 0,053
Post-treatment	0,965 ± 0,257	0,479 ± 0,112	-0,149 ± 0,142	0,373 ± 0,109	0,260 ± 0,048	-0,220 ± 0,076	-9,900 ± 3,262	-4,145 ± 0,073	0,538 ± 0,060

In Table 1, we report the results of the mean values and standard deviation of the generalized Hurst exponents h(2),$\Delta\alpha$, Δf, A, B, C, Δh, $\Delta\alpha_L$, $\Delta\alpha_R$, in the condition of pre-treatment, during the NPT treatment and post- treatment.

The use of the Generalized Hurst Exponents and the other indices represent a particular tool of the multifractal analysis. Concerning our NPT analysis, we observe that their values, in the passage from at rest to NPT exercise, and after returning to the at rest condition, implies a modification of the values of such indices that, therefore, represent fundamental elements to characterize the physiological condition of the investigated muscles. We have the range of normality as they are given by their mean values plus standard deviation. After we have the mean values and standard deviation during the NPT treatment.

Such results indicate the modification of the muscle regime during the NPT and the transitions of such muscle dynamics during the NPT and the importance of using such multifractal indices, in general, in current sEMG studies owing to their sensitivity to the physiological conditions of the muscles. Such indices modify their values during the NPT treatment and after they return to normal values. It is this datum that confirms the effectiveness of our treatment. In fact, the passage of such indices indicates that the NPT is an effective treatment that rearranges the physiological dynamics of the muscle.

$\Delta\alpha_L$ and $\Delta\alpha_R$ evidence a rather constant regime of the fluctuations ranging $\Delta\alpha_L$ from 0.304 ± 0.039 to 0.412 ± 0.034 and to 0.439 ± 0.115 for the right trapezius in the experimental conditions of pre-, during- and post-NPT treatment, passing from 0.304 ± 0.039 to 0.237 ± 0.139 to 0.503 ± 0.157 in the phases pre-, during- and post-NPT treatment for the left trapezius, from 0.434 ± 0.141 to 0.385 ± 0.079, to 0.512 ± 0.132 in the phases of pre-, during- and post- treatment for the right abdominals, to 0.391 ± 0.078 to 0.246 ± 0.106 to 0.389 ± 0.083 in the phases of pre-, during- and post-NPT treatment for the left abdominals, and, finally, for 0.200 ± 0.087 to 0.464 ± 0.169 to 0.523 ± 0.016 in the phase of pre-, during- and post-NPT treatment for the right adductors and 0.280 ± 0.117 to 0.426 ± 0.129 to 0.260 ± 0.048 on the phases of pre-, during- and post-NPT treatment for the left adductors. $\Delta\alpha_R$ vary from - 0.207 ± 0.055 to -0.284 ± 0.036 to -0.407 ± 0.049 in the phases pre-, during- and post-NPT treatment for the right trapezius, from -0.207 ± 0.055, to -0.207 ± 0.088, to -0.454 ± 0.022 in pre-, during- and post-NPT treatment for the left trapezius, from -0.471 ± 0.130 to -0.357 ± 0.116 to -0.522 ± 0.052 in the phases of pre-, during- and post-NPT treatment for the right abdominals and from -0.461 ± 0.016 to -0.234 ± 0.091 to -0.405 ± 0.098 in the phase of

pre-, during- and post-NPT treatment for the left abdominals, and from -0.174 ± 0.059, to -0.438 ± 0.063 to -0.316 ± 0.110 in the phases of pre-, during- and post-NPT treatment for the right adductors and from -0.255 ± 0.070, to -0.296 ± 0.052 to -0.220 ± 0.076 in the phases of pre-, during- and post-NPT treatment for the left adductors.

Next, an examination will be made of the behavior of the multifractal spectrum $f(\alpha)$ and the Δf. $f(\alpha)$ was fitted by a parable with the coefficients A, B, C as explained in detail in the text. For the right trapezius we find A = - 8.281 ± 1.182, B = -3.472 ± 0.880, C = 0.674 ± 0.161 in the condition at rest and pre-NPT treatment. This regime evolves through new transitions to A = - 5.798 ± 0.557, B = - 3.418 ± 0.058 and C = 0.534 ± 0.004 during the NPT treatment and to A = - 4.064 ± 1.782, B = - 3.200 ± 0.982, C = 0.444 ± 0.134 in the phase of post-NPT treatment.

Again, the data on $f(\alpha)$ confirms that for the multifractal spectrum, we have a regime of total rearrangement of the condition of multifractality in passing from the pre- to during and post-NPT treatment with statistically significant differences. For the left trapezius, we have A = - 4.212 ± 1.379. B = - 3.024 ± 0.350, C = 0.511 ± 0.040 in the phase of pre-NPT treatment and it becomes A = - 14.666 ± 8.432, B = - 4.991 ± 1.236, C = 0.555 ± 0.075 during the NPT treatment and A= - 2.894 ± 0.310, B = - 2.692 ± 0.432 and C = 0.436 ± 0.093 in the at rest post-NPT treatment. Through this data we confirm again that, by the NPT treatment, we have a total regime of multifractality that is during the pre and post-NPT treatment and during the NPT treatment with transitions of this multifractality regime that is signed from the reported values of A, B, and C.

In the right abdominals, we have A = - 3.518 ± 1.269, B = - 3.078 ± 0.275, C = 0.383 ± 0.103 at rest before the NPT treatment, A = - 4.831 ± 1.313, B = - 3.240 ± 0.389, C = 0.477 ± 0.223 during the NPT treatment and A = - 3.166 ± 0.469, B = -3.260 ± 0.152, C = 0.267 ± 0.031 in the at rest, post the NPT treatment. In the left abdominals, it is instead A = -3.190 ± 0.190, B = - 2.972 ± 0.098, C = 0.391 ± 0.014 in the pre-NPT treatment, A = -9.725 ± 5.281, B = - 2.434 ±3.699, C = 0.593 ± 0.095 during the NPT treatment and A = - 4.240 ± 1.253, B = - 3.311 ± 0.203 and C = 0.396 ± 0.104 in the at rest, post NPT treatment.

For the right adductors, we have instead, for the right, A = -10.930 ± 2.020, B = - 2.526 ± 3.934, C = 0.679 ± 0.230 at rest, pre-NPT treatment, A = - 3.907 ± 1.194, B = - 3.297 ± 0.626, C = 0.384 ± 0.064 during the NPT treatment and A = -3.991 ± 0.135, B = -2.560 ± 0.843, C = 0.590 ± 0.256 in the post-NPT treatment.

For the left adductors, we have instead A = - 8.495 ± 4.328, B = - 3.984 ± 0.968, C = 0.576 ± 0.009 in the pre-NPT treatment, A = -5.402 ± 2.400, B = - 3.069 ± 0.777, C = 0.600 ± 0.053 during the NPT treatment and A=-9.900 ± 3.262, B = - 4.145 ± 0.073, C = 0.538 ± 0.060 in the regime of the at rest, post-NPT treatment.

Looking to the nonlinear behavior of the curves, we conclude that all the recorded signals exhibit a multifractal regime. In particular, the behavior of $f(\alpha)$, the multifractal spectrum, confirms that we are in the presence of a multifractal regime in all the recorded channels relating the right and left trapezius, the right and left adductors and the right and left abdominal muscles. We pass to the next step, the surrogate data analysis. We calculated $F_q(s)$ against s and we performed the Surrogate Data Analysis by calculating the AutoCorrelation Function (ACF), h(q) against q and the multifractal spectrum of the data and their Surrogate. The results are reported in Figures 4-8.

Let us take a look at the statistical analysis. By this statistical analysis, we have significant results for h(2) for the left trapezius. For $\Delta\alpha$, we have significant results for the left trapezius and the left abdominals. For Δf, we obtain significant results for the right trapezius. For Δh, significant results are obtained for the left trapezius and the left abdominals. ΔaL as well as ΔaR give statistical significance for the left abdominals. The coefficients A, B and C are statistically significant for the left trapezius and left abdominals. The level of significance is reported in Table 2 with stars.

The outcome and significance of the used indices become self-evident, if we think that the athletes obtained a significant rearrangement of such indices during the NPT treatment with a subsequent return to their normal conditions after the NPT Treatment. The datum evidences, consequently, that the NPT treatment modifies such parameters with a given significance and that they return to be normal after the NPT Treatment.

4. Discussion

In this section we give a look at the h(2) and $\Delta h = h(q_{min})-h(q_{max})$ values. The human body system needs to be functioning in a coordinated manner where no privileged point of observation is able to be observed. This means that regardless of where you look at the system and what instrument you measure the system with, it should likely be similar across all scales. Energy and information need to be evenly distributed to all parts of the system. In the case of a disease or disorder, this is not the case.

Table 2. Results of statistical analysis, repeated-measures ANOVA, for h(2), Δα, Δf, A, B, C, Δh, $\Delta\alpha_L$, $\Delta\alpha_R$ comparing the indices in the conditions of pre-, during- and post-treatment

	H(2)	Δα	**Δf**	**Δh**	**ΔαL**	**ΔαR**	**A-B-C**
CH1 (right trapezius)							
P value	1	1	0,0260	1	1	1	1
P value summary	ns	ns	*	ns	ns	ns	ns
P < 0.05	No	No	Yes	No	No	No	No
F	-2,1610	-2,2720	10,4100	-2,3330	-2,2330	-2,4440	-2,2420
R squared	13,4200	8,3550	0,8388	7,0120	9,5880	5,5100	9,2590
CH2 (left trapezius)							
P value	P<0.0001	0,0104	0,8057	0,0049	0,0709	0,0021	0,0297
P value summary	***	*	Ns	**	ns	**	*
P < 0.05	Yes	Yes	No	Yes	No	Yes	Yes
F	28,8500	7,4590	0,2208	9,4850	3,4890	12,1800	5,1030
R squared	0,8523	0,5987	0,04228	0,6548	0,4110	0,7089	0,5051
CH3 (right abdominals)							
P value	1	1	0,3724	1	1	1	1
P value summary	ns	ns	Ns	ns	ns	ns	ns
P < 0.05	No	No	No	No	No	No	No
F	-9,2270	-3,7840	1,1700	-3,8150	-3,7080	-3,9780	-3,6700
R squared	2,1830	4,8290	0,2806	4,6810	5,2370	4,0680	5,4780
CH4 (left abdominals)							
P value	1	0,0096	0,1557	0,0114	0,0165	0,0084	0,0356
P value summary	ns	**	ns	*	*	**	*
P < 0.05	No	Yes	No	Yes	Yes	Yes	Yes
F	-7,6530	8,7910	2,3670	8,2390	7,1590	9,2180	5,2070
R squared	2,0950	0,6873	0,3718	0,6732	0,6415	0,6974	0,5655

Table 2. (Continued)

	H(2)	Δα	**Δf**	**Δh**	Δα**L**	Δα**R**	**A-B-C**
CH5 (right adductors)							
P value	1	1	0,4633	1	1	1	1
P value summary	ns	ns	ns	ns	ns	ns	ns
P < 0.05	No	No	No	No	No	No	No
F	-4,2500	-1,0870	1,1580	-1,0950	-1,1030	-1,1360	-2,8340
R squared	3,4000	12,4900	0,5367	11,5700	10,7100	8,3300	3,3980
CH6 (left adductors)							
P value	1	1	1	1	1	1	1
P value summary	ns	ns	ns	ns	ns	ns	ns
P < 0.05	No	No	No	No	No	No	No
F	-2,4670	-4,1250	-1,7070	-3,2920	-3,2820	-8,0990	-3,6690
R squared	5,2810	3,6670	2,4150	11,2800	11,6500	2,6140	2,1980

The raw sEMG data harvested from the trapeze, abdominals and adductors should all look the same or very similar so that when an event occurs at one location the same event can be observed at the other locations at the same time scale simultaneously. When this level of synchronicity is not being observed in the time series, then this is indicative of a system harbouring a disease or disorder (even without knowledge of patients' medical history). However, as the patient engages with the NPT process in the following days, the system displays much more deterministic behaviors of motor units across all scales (channels) as visually evidenced in their time series portraits in the absence of analyses.

The generalized Hurst Exponent h(2), and $\Delta h = h(q_{min})-h(q_{max})$ will first be discussed in this section. Different q values have varying effects on the fluctuation functions. The positive q segment ν with large variance describes the scaling behavior of the segments with large fluctuations and, in general, large fluctuations are characterized by a smaller scaling exponent for multifractal time series. For negative q, segments ν with small variance will dominate the average F(ν). Thus, if q is negative, the scaling exponent describes the scaling behavior of segments with small fluctuations, usually characterized by a larger scaling exponent.

In Table 1, we see that we have values of h(2) greater than 0.5 in the case of pre-treatment at rest and during NPT for the Ch1 (right trapezius) and the results are greater than 0.5 in pre-, during- and post-treatment in channels ch2 (left trapezius), ch3 (right abdominals), ch4 (left abdominals), ch5 (right adductors), and ch6 (left adductors). For ch1 and ch2, the values of h(2) are about 0.5 during the NPT treatment and are less of 0.5 in the post-NPT treatment. Values greater than 0.5 indicate that the time series have long-term, correlated and persistent fluctuations. Conversely, values of h(2) that are less than 0.5 indicate that we are in presence of a time-series in which the fluctuations are anti-persistent. Values of h(2) around 0.5 instead indicate a completely uncorrelated series. However, the value applicable to series for which the autocorrelations at small time lags can be positive or negative but where the absolute values of the autocorrelations decay exponentially quickly to zero.

In conclusion, starting with the analysis of the generalized Hurst exponent h(2) and $\Delta h= h(q_{min})-h(q_{max})$, we can conclude that there are modifications of the multifractal regime during the NPT treatment respect to the pre and post treatment with a drastic change of the multifractal regime that passes from the stationary, correlated and persistent fluctuations in the phase of at rest pre-

treatment to the phase of uncorrelated signal in the phase of the NPT treatment to the regime of short term, non-stationary, intermittent and non-persistent behavior during post-NPT treatment for the cases of trapezius channels (Ch1 and Ch2). We pass from the value of $h(2) = 0.796 \pm 0.084$ for the pre-treatment to the value of $h(2) = 0.551 \pm 0.026$ during the NPT treatment and to $h(2) = 0.472 \pm 0.047$ for the post-treatment for right trapezius and to the values of $h(2) = 0.669 \pm 0.129$ in the phase of the pre-treatment to the value of $h(2) = 0.546 \pm 0.160$ during the treatment and to the value $h(2) = 0.589 \pm 0.167$ for the post- treatment for the left trapezius. For the other channels relating the abdominals and the adductors (the other channels Ch3, Ch4, Ch5 and Ch6) for the transitions we move in the direction of the stationary, correlated, and persistent fluctuations but with different values of h(2) and Δh in the case of pre-NPT treatment respect to the situation of during and post-NPT treatment.

With regard to α, $\Delta\alpha$, $\Delta\alpha_R$, and $\Delta\alpha_L$, the behavior of alpha is nonlinear in all the case examined of alpha pre-, during- and post-NPT treatment in the trapezius, adductors, and abdominals. The width $\Delta\alpha$ of a multifractal spectrum provides a measure of multifractality: a larger range of $\Delta\alpha$ indicates a wider multifractal spectrum, implying a higher degree of multifractality. A larger or smaller multifractal signal (corresponding to a larger or smaller $\Delta\alpha$) implies a greater or lesser heterogeneous signal. A signal is heterogeneous if it is characterized by sudden bursts of high frequency, intermittencies and/or irregularities, respectively. $\Delta\alpha_L$ and $\Delta\alpha_R$ are the left- and right-hand branches of the multifractal spectrum curve; their values describe the distribution patterns of high and low fluctuations, respectively [27,28]. The asymmetry index (R), which ranges from -1 to 1, quantifies the deviations of the multifractal spectrum curve [29].

For the right trapezius, we have $\Delta\alpha = 0.512 \pm 0.059$ in the phase of pre-NPT treatment, $\Delta\alpha = 0.696 \pm 0.002$ during the NPT treatment and $\Delta\alpha = 0.846 \pm 0.163$ in the phase of post-NPT treatment. In substance we obtain an increment of multifractality passing from pre to the post- treatment.

The behavior is different for the left trapezius, passing from $\Delta\alpha = 0.694 \pm 0.169$ in the pre-treatment test to $\Delta\alpha = 0.444 \pm 0.227$ during the NPT treatment and $\Delta\alpha = 0.957 \pm 0.137$ in the phase of post-NPT treatment. Indeed, in the right trapezius, we have an increase of multifractality in passing from the pre-, to during- and to post- treatment, while instead in the left trapezius, we have a reduction of multifractality in passing from the pre-, to during- the treatment and increasing multifractality in the regime of post-NPT treatment.

For the right abdominals, we have instead $\Delta\alpha = 0.905 \pm 0.267$ in the phase of pre-NPT treatment, to $\Delta\alpha = 0.742 \pm 0.183$ during the NPT treatment and $\Delta\alpha = 1.034 \pm 0.183$ in the post-NPT treatment. We have a reduction of multifractality passing from pre to during the NPT treatment and an increase of multifractality passing from the pre or during NPT treatment to post-NPT treatment. For the left abdominals, we have $\Delta\alpha = 0.853 \pm 0.090$ in the pre-NPT treatment, $\Delta\alpha = 0.479 \pm 0.190$ during the treatment and $\Delta\alpha = 0.794 \pm 0.181$ in the post-NPT treatment. We obtain again a diminution of the multifractals in passing from the pre to during the NPT treatment and an increase in multifractality going from the phase of during the NPT treatment to the regime of post the NPT treatment.

For the right adductors, we have $\Delta\alpha = 0.373 \pm 0.031$ for the pre-treatment, $\Delta\alpha = 0.901 \pm 0.228$ during the NPT treatment and $\Delta\alpha = 0.840 \pm 0.095$ during the post- treatment.

The left adductors show instead $\Delta\alpha = 0.534 \pm 0.187$ in the pre-treatment condition, $\Delta\alpha = 0.722 \pm 0.174$ during the NPT treatment and $\Delta\alpha = 0.479 \pm 0.112$ in the post-NPT treatment. For the right and left adductors, we have an increase of multifractality in passing from the pre-NPT treatment to during the NPT treatment and a reduction in passing from the during the NPT treatment to the post-NPT treatment.

In conclusion, we have a continuous regime of rearrangement of the dynamics of multifractality in the trapezius, in the abdominals and the adductors during the pre-NPT and post-NPT treatment.

We deduce that the NPT treatment, modifying the multifractal regime, induce in all the trapezius, abdominals and adductors, modifications that are reflected also in the pre-, during- and post-treatment in the different values of the coefficients A, B, C, that reflect the multifractal spectrum $f(\alpha)$.$\Delta f(\alpha)$ is the difference between the maximum and minimum values of $f(\alpha)$. The difference $\Delta f(\alpha)$ between maximum and minimum values of the singularity provides an estimate of the spread in changes in fractal patterns. Since $\Delta f(\alpha)$ denotes the frequency ratio of the largest to the smallest fluctuation, $\Delta f(\alpha) > 0$ means that the largest fluctuations are more frequent than smallest fluctuations, while $\Delta f(\alpha) < 0$ is the reverse. It is evident from the data of Table 1 that $\Delta f(\alpha)$ are all negative for right trapezius, and for the abdominals, both right and left, while it is positive for the right adductors. For the left trapezius it starts to be positive at rest, pre-NPT treatment, and becomes negative in the NPT treatment and in post-NPT treatment. The same thing happens for the right abdominals. This is

the situation of the rearrangements of the multifractal spectrum following the transitions that are induced from the NPT treatment.

In the statistical analysis, the results are significant for h(2) in the left trapezius, for $\Delta\alpha$ in the left trapezius and the left abdominals, for Δf in the right trapezius, Δh in the left trapezius and the left abdominals and for $\Delta\alpha_L$ and $\Delta\alpha_R$ in the left trapezius and left abdominals. The coefficients A, B and C, are statistically significant for the left trapezius and left abdominals. The level of significance is reported with stars in Table 2.

Conclusion

Surface electromyography (sEMG), the nonlinear summation of the electrical activity of the motor units in a muscle which reflects the state of neuromuscular function, has been widely applied to disease diagnosis, pathologic analysis, and rehabilitation evaluation [30–32]. Traditional linear and statistical analysis methods have some significant limitations due to the short-term stationary and lower signal-noise ratio of sEMG, but it is mixed to the nonlinear regime that gives us the main feature of the signal [33].

The basic feature of the linear regime may be analyzed by the Fourier Transform (FFT) with estimation of other linear indexes such as the Muscle Response and the Muscle Fatigue indexes. However, sEMG displays chaotic features and muscle fatigue results in reduced complexity [34] . In this paper, we report multifractal analysis into the field of sEMG process to investigate this dynamical regime: the sEMG on the bilateral masseter, levator labii superioris and frontalis in athletes was recorded. Generally speaking, also the chaotic analysis should have been employed to extract new features, including correlation dimension, Lyapunov exponent, and entropy to indicate in an explicit way that, according to our analysis, the sEMG is multifractal, and chaotic. Consequently, chaotic analysis and multifractal analysis could provide a new insight into the study of the complexity of the EMG and the analysis of multifractality and chaoticity of such a signal could help to analyze the system itself, in particular, the dynamics of modifications found between discrete system's states. The multifractal analysis, that is characteristic of the complexity of the curve, can be computed directly in the time domain by using some algorithms specifically developed. Other studies have shown that the fractal dimension of EMG is sensitive to magnitude and rate of muscle force generated [35–37] and the fractal dimension correlates to the muscle's

potential in athletics. The better the athlete is, the higher the fractal dimension. The fractal dimension is representative of the training level. The purpose of this work was to study, in terms of multifractal analysis and to show how the sEMG signals are generated in trapezius, adductors and abdominals pre-, during- and post-NeuroPhysics Treatment providing experimental support to the thesis elaborated in Ross and Ware's previous work [1]. From a clinician and medical perspective, a net modification in the dynamics of the recorded signals may be observed during the treatment. As illustrated by Table 1, we have executed the multifractal analysis of the recorded signals and derived the indices of the Generalized Hurst Exponent, the Generalized Multifractal Dimension, the Fractal Spectrum, and the indices Δh, $\Delta\alpha$, $\Delta\alpha_{\Lambda}$, $\Delta\alpha_{R}$, $f(\alpha)$, $\Delta\phi(\alpha)$.

All such indices have enabled us to conclude that the sEMG signals are differentiated at rest and during NPT treatment but remain as multifractals. Often the calculated indices show a statistical significance difference between at rest and NPT treatment or in the (left and right) trapezius and (left and right) adductors or between adductors (left or right) and abdominals (left and right).

All these results have been reported in the table of statistical analysis for which we have employed the method of Anova. The scheme of the arising model is as follows: all the muscles, trapezius, abdominal, and adductors represent complex systems whose bio signal profiles, recorded by the sEMG, constitute a multifractal.

These systems are subjected to continuous transitions during the NPT treatment which enable a continuous and differential rearrangement of the indices between different muscles or between the same muscles during the treatment. Such transitions are finalized to maintain such multifractal regime in the muscles. The multifractality, therefore, remains the principal objective of the muscle dynamics that rearranges itself in the occasion of the treatment to maintain such behavior during the phases of pre-, during- and post-treatment. Therefore, we conclude that the exact dynamics of the trapezius, abdominals and adductors is that one of fractality that by continuous transitions, rearrange continuously their dynamics. The attractors of such systems are continuously moving in their inner structure to enable modifications of their structure by transitions that we see by a modification of the multifractal regime.

In conclusion, when performed across all patients of interest, multifractal analysis enables consistency to be accomplished and established. Multifractal analysis of electrophysical data harvested from all patients of interest on day

1 pre-NPT can be performed as a baseline measurement and can then be compared against the multifractal analysis performed on the EMG data from the healthy elite athletes portrayed in this submission.

Author Contributions

Conceptualization, F.C., F.S., R.M., K.W. and E.C.; methodology, F.C., F.S., R.M., K.W. and E.C.; Software, F.C., F.S., R.M., K.W. and E.C.; Validation, F.C., F.S., R.M., K.W. and E.C.; Formal analysis, C.R., F.K., F.C., F.S., R.M., K.W. E.C. and A.D.L.; Investigation, C.R., F.C., F.S., R.M., K.W., E.C. and A.D.L.; Resources, K.W. and E.C.; Data Curation, C.R., F.K.; F.C., F.S., R.M., K.W. and E.C.; Writing—Review & Editing, C.R., F.K., F.C., F.S., R.M., K.W., E.C. and A.D.L.; Visualization, C.R., F.K., F.C., F.S., R.M., K.W., E.C. and A.D.L.; Supervision, C.R., F.K., F.C., F.S., R.M., K.W., E.C. and A.D.L.; Project Administration, C.R., F.K., F.C., F.S., R.M., K.W., E.C. and A.D.L. All authors have read and approved the final version of the manuscript.

Acknowledgments

The authors declare they have no conflict of interest with this work. This research received no external funding. Informed consent was obtained from all subjects involved in the study. The participants (trained athletes) were clients of the NeuroPhysics Therapy Clinic. Collecting electrophysiological data from all clients/patients was approved as a standard procedure by the Association for Practising Neurotricians and Neurotricionists (APNN) (protocol code APNN-2013-0214 and date of approval 10-Feb-2014). Data is available on request. Pre-, during- and post-NPT data from various sources are stored, inclusive of fine-grained gait and stance analysis using Zebris technology at the Institute Neurotricional Sciences, Australia. AusIndustry-Science and Technology Department audits the Institute Neurotricional Sciences every year and data management and patient privacy are also covered in the audit.

References

[1] Namazi, H. (2021). Complexity-Based Analysis of the Correlation between Stride Interval Variability and Muscle Reaction at Different Walking Speeds. *Biomed. Signal Process. Control*, 69, 102956.

[2] Namazi, H. (2019). Decoding of Hand Gestures by Fractal Analysis of Electromyography (Emg) Signal. *Fractals*, 27, 1950022.

[3] Beretta Piccoli, M., Boccia, G., Ponti, T., Clijsen, R., Barbero, M., and Cescon, C. (2018). Relationship between Isometric Muscle Force and Fractal Dimension of Surface Electromyogram. *Biomed Res Int*, 2018, 5373846.

[4] Ross, S. N., and Ware, K. (2013). Hypothesizing the Body's Genius to Trigger and Self-Organize Its Healing: 25 Years Using a Standardized Neurophysics Therapy. *Front. Physiol.*, 4 NOV, doi:10.3389/fphys.2013.00334.

[5] Morrison, S., and Sosnoff, J. J. (2010). The Impact of Localized Fatigue on Contralateral Tremor and Muscle Activity Is Exacerbated by Standing Posture. *Electromyogr Kinesiol*, 20, 1211–1218.

[6] Fink, P. W., Kelso, S., Jirsa, V. K., and De Guzman, G. (2000). Recruitment of Degrees of Freedom Stabilizes Coordination. *J. Exp. Psychol. Hum. Percept. Perform.*, 26, 671–692, doi:10.1037/0096-1523.26.2.671.

[7] Fuchs, A., and Jirsa, V. K. (2000). The HKB Model Revisited: How Varying the Degree of Symmetry Controls Dynamics. *Hum Mov Sci*, 19, 425–449.

[8] West, B. (2013). *Fractal Physiology and Chaos in Medicine*; 2nd ed.; World Scientific, Singapore.

[9] Hong, S., Bodfish, J., and Newell, K. (2006). Power Law-Scaling for Macroscopic Entropy and Microscopic Complexity: Evidence from Human Movement and Posture. *Chaos*, 16, 013135.

[10] Rogers, B., Gronwald, T., and Mourot, L. (2021). Analysis of Fractal Correlation Properties of Heart Rate Variability during an Initial Session of Eccentric Cycling. *Int J Env. Res Public Heal.*, 18, 10426.

[11] Lipsitz, L. A. (2008). Dynamic Models for the Study of Frailty. *Mech Ageing Dev*, 128, 675–676.

[12] Seely, A. J. E., and Macklem, P. (2012). Fractal Variability: An Emergent Property of Complex Dissipative Systems. *Chaos*, 22, 013108.

[13] Heffernan, K. S., Sosnoff, J. J., Jae, S. Y., Gates, G. J., and Fernhall, B. (2008). Acute Resistance Exercise Reduces Heart Rate Complexity and Increases QTc Interval. *Int. J. Sports Med.*, 29, 289–293, doi:10.1055/s-2007-965363.

[14] Izquierdo, I., Bevilaqua, L. R. M., Rossato, J. I., Bonini, J. S., Medina, J. H., and Cammarota, M. (2006). Different Molecular Cascades in Different Sites of the Brain Control Memory Consolidation. *Trends Neurosci.*, 29, 496–505, doi:10.1016/ j.tins.2006.07.005.

[15] Burggren, W. W., and Monticino, M. G. (2005). Assessing Physiological Complexity. *J. Exp. Biol.*, 208, 3221–3232, doi:10.1242/JEB.01762.

[16] Kelso, J. A. S. (1995). *Dynamic Patterns: The Self-Organization of Brain and Behavior*; MIT Press, Cambridge, MA, U.S.A.

[17] Iberall, A. S., and Soodak, H. (1998). *Primer on Homeokinetics: A Physical Foundation for Complex SystemsNo Title*; Cri-de-Coeur Press, Laguna Woods, California.

[18] Tsuda, I. (2009). Hypotheses on the Functional Roles of Chaotic Transitory Dynamics. *Chaos*, 19, doi:10.1063/1.3076393.

[19] Kaneko, K., and Tsuda, I. (2003). Chaotic Itinerancy. *Chaos*, 13, 926–936.

[20] Thelen, E., and Smith, L. B. (1994). *A Dynamic Systems Approach to the Development of Cognition and Action*; MIT Press, Cambridge, Massachusetts.

[21] Matthews, P. C., R. E., M., and Strogatz, S. H. (1991). Dynamics of a Large System of Coupled Nonlinear Oscillators. *Phys. D Nonlinear Phenom.*, 52.

[22] Cross, M. C., and Hohenberg, P. C. (1993). Pattern Formation Outside of Equilibrium. *Rev Mod Phys*, 65, 851–1112.

[23] Buchanan, J. J. (1993). Posturally Induced Transitions in Rhythmic Multi Joint Limb Movements. *Exp Brain Res*, 94, 131–142.

[24] Marri, K., and Swaminathan, R. (2015). Analyzing Origin of Multifractality of Surface Electromyography Signals in Dynamic Contractions. *J. Nanotechnol. Eng. Med.*, 6, 031002.

[25] Trybek, P., Nowakowski, M., and Machura, L. (2018). Multifractal Characteristics of External Anal Sphincter Based on SEMG Signals. *Med. Eng. Phys.*, 55, 9–15, doi:10.1016/j.medengphy.2018.03.007.

[26] Wang, F., Yang, Z., and Wang, L. (2016). Detecting and Quantifying Cross-Correlations by Analogous Multifractal Height Cross-Correlation Analysis. *Phys. A Stat. Mech. its Appl.*, 444(C), 954–962.

[27] Agterberg, F. P. (2001). Multifractal Simulation of Geochemical Map Patterns. In *Geologic modeling and simulation: sedimentary systems*; Merriam, D.F., Davis, J.C., Eds.; Kluwer Academic & Plenum Publishers: New York, pp. 327–346.

[28] Eversetz, C. J. G., and Mandelbrot, B. B. (1992). Multifractal Measures. In *Chaos and Fractals*; Peitgen, H.O., Jurgens, H., Saupe, D., Eds.; Springer: New York, pp. 922–953.

[29] Xie, S., and Bao, Z. (2004). Fractal and Multifractal Properties of Geochemical Fields. *Math. Geol. 367*2004, 36, 847–864, doi:10.1023/B:MATG.0000041182.70233.47.

[30] Marri, K., and Swaminathan, R. (2016). Classification of Muscle Fatigue Using Surface Electromyography Signals and Multifractals. In *Proceedings of the 2015 12th International Conference on Fuzzy Systems and Knowledge Discovery*, FSKD 2015; Institute of Electrical and Electronics Engineers Inc., January 13; pp. 669–674.

[31] Marri, K., and Swaminathan, R. (2015). Analysis of Biceps Brachii Muscles in Dynamic Contraction Using SEMG Signals and Multifractal DMA Algorithm. *Int. J. Signal Process. Syst.*, 4, doi:10.12720/ijsps.4.1.79-85.

[32] Chatterjee, S., Roy, S. S., Bose, R., and Pratiher, S. (2020). Feature Extraction from Multifractal Spectrum of Electromyograms for Diagnosis of Neuromuscular Disorders. *IET Sci. Meas. Technol.*, 14, 817–824, doi:10.1049/iet-smt.2019.0132.

[33] Arjunan, S. P., and Kumar, D. (2007). Fractal Theory Based Non-Linear Analysis of SEMG.; *Proc. 3rd International Conference on Intelligent Sensors, Sensor Networks and Information*, pp. 545–548.

[34] Rampichini, S., Vieira, T. M., Castiglioni, P., and Merati, G. (2020). Complexity Analysis of Surface Electromyography for Assessing the Myoelectric Manifestation of Muscle Fatigue: A Review. *Entropy*, 22, doi:10.3390/E22050529.

[35] Wang, G., Ren, X. M., Li, L., and Wang, Z. Z. (2007). Multifractal Analysis of Surface EMG Signals for Assessing Muscle Fatigue during Static Contractions. *J. Zhejiang Univ. Sci. A*, 8, 910–915, doi: 10.1631/jzus 2007.A0910.

[36] Wang, G., and Ren, D. (2013). Classification of Surface Electromyographic Signals by Means of Multifractal Singularity Spectrum. *Med Biol Eng Comput*, 51, 277– 284, doi: 10.1007/s11517-012-0990-9.

[37] Marri, K., and Swaminathan, R. (2015). Identification of Onset of Fatigue in Biceps Brachii Muscles Using Surface EMG and Multifractal DMA Algorithm. In *Proceedings of the 52nd Annual Rocky Mountain Bioengineering Symposium and 52nd International ISA Biomedical Sciences Instrumentation Symposium 2015*, pp. 109–116.